Article ID: 1000-7032(2022)09-1459-10

Spectroscopic Properties of Ni^{2+} Ions in Octahedral Complexes

BRIK Mikhail G[1,2,3,4*], KURBONIYON Mekhrdod S[1], MA Chong-geng[1*]

(1. *School of Optoelectronic Engineering & CQUPT-BUL Innovation Institute, Chongqing University of Posts and Telecommunications, Chongqing* 400065, *China*;
2. *Institute of Physics, University of Tartu, Tartu* 50411, *Estonia*;
3. *Faculty of Science and Technology, Jan Długosz University, PL*-42200 *Częstochowa, Poland*;
4. *Academy of Romanian Scientists, Bucharest* 050044, *Romania*)

* *Corresponding Authors, E-mail: mikhail. brik@ut. ee; macg@cqupt. edu. cn*

Abstract: Based on an up-do-date literature data, we consider an empirical trend between the energy of the spin-forbidden $^3A_2$-^1E transition of the octahedrally coordinated Ni^{2+} ions and a new nephelauxetic parameter $\beta_1 = \sqrt{\left(B/B_0\right)^2 + \left(C/C_0\right)^2}$ (B, C (B_0, C_0) are the Racah parameters of Ni^{2+} ions in a crystal(free state), respectively). It is demonstrated that the energy of the Ni^{2+} ^1E state is a linear function of the β_1 parameter. These findings prove importance of a simultaneous consideration of reduction of both Racah parameters B and C due to the nephelauxetic effect. Such an approach is more accurate in estimating the energy position of the ^1E level. The commonly used nephelauxetic ratio $\beta = B/B_0$, which completely ignores the reduction in the values of the Racah parameter C, is not accurate enough for this purpose. The collected in the present paper experimental data and their analysis can be useful for researchers working with the crystalline materials doped with Ni^{2+} ions.

Key words: Ni^{2+}; spin-forbidden transitions; covalency

CLC number: O482. 31 **Document code**: A **DOI**: 10. 37188/CJL. 20220243

八面体配合物中 Ni^{2+} 离子的光谱性质

BRIK Mikhail G[1,2,3,4*], KURBONIYON Mekhrdod S[1], 马崇庚[1*]

(1. 重庆邮电大学 光电工程学院 &“重庆邮电大学-伦敦布鲁内尔大学”交叉创新研究院, 重庆 400065;
2. 塔尔图大学 物理研究所, 爱沙尼亚 塔尔图 50411;
3. 琴斯托霍瓦师范大学 科学与技术学院, 波兰 琴斯托霍瓦 42200;
4. 罗马尼亚国家科学院, 罗马尼亚 布加勒斯特 050044)

摘要: 基于最新的文献数据,我们研究了八面体配位下 Ni^{2+} 离子自旋禁止跃迁 $^3A_2$-^1E 的能量与新的电子云膨胀效应参数 $\beta_1 = \sqrt{\left(B/B_0\right)^2 + \left(C/C_0\right)^2}$ 之间的经验关系,其中(B、C)和(B_0、C_0)分别是 Ni^{2+} 离子在晶体中和自由离子状态下描述3d电子间库仑作用的拉卡参数。研究结果表明,Ni^{2+} 离子 ^1E 态的能量是 β_1 参数的线性函数。这样的发现确认了完全处理电子云膨胀效应需要同时考虑两个拉卡参数 B 和 C 约减贡献的重要事实。通常

收稿日期: 2022-06-06; **修订日期**: 2022-07-04
基金项目: 国家科技部外专局“一带一路”创新人才交流外国专家项目(DL2021035001L); 2021年度中国博士后科学基金国外交流引进项目(重庆专项); 国家自然科学基金(52161135110)资助项目
Supported by National Foreign Experts Program for “Belt and Road Initiative” Innovative Talent Exchange(DL2021035001L); 2021 Chongqing Postdoctoral International Exchange Program of China Postdoctoral Science Foundation; National Natural Science Foundation of China(52161135110)

使用的电子云膨胀效应参数$\beta = B/B_0$由于完全忽略了拉卡参数C的约减贡献，在估计^{1}E态能级位置上是不准确的。相比而言，我们构建的理论方法则更好。本文所收集的实验数据以及实施的理论分析均将会对Ni^{2+}离子掺杂材料的光谱学研究有一定的参考价值。

关 键 词：Ni^{2+}；自旋禁戒跃迁；共价性

1 Introduction

Theoretical and experimental studies of the transition metal (TM) ions spectroscopic properties in a free state and in solids are still actively being performed, which can be readily explained by numerous applications in science and technology[1-3]. In particular, the TM ions with an unfilled 3d electron shell are of special importance. These ions can be stabilized in solids in different oxidation states and in different coordination, and this circumstance contributes to the variety and complexity of the optical spectra of these ions in various crystalline materials. Since the 3d electron shell is the outer one, its electrons strongly interact with nearest neighbors in the crystal lattice. The overall appearance of the absorption and luminescence spectra of these TM ions is determined by a combination of the spin-allowed broad emission bands and narrow spin-forbidden peaks. The former ones are used for getting tunable laser generation[4], whereas the latter ones are important for lighting[5-8], as well as for lasing (like ruby laser that operates on the sharp spin-forbidden ^2E-$^4A_2$ emission transition of Cr^{3+} ions).

One of those 3d TM ions is a divalent nickel, Ni^{2+}, with its $3d^8$ electron configuration. An interest to this ion has been revived recently because of its infrared emission in the second (1 000−1 350 nm) and third (1 550−1 870 nm) biological windows[9-11], which facilitates applications of these ions in optical thermometry and bioimaging.

The Ni^{2+} electron configuration ($3d^8$) in terms of the number of allowed states is equivalent to the $3d^2$ electron configuration. Both configurations have 45 allowed microstates, which obey the Pauli exclusion rule. These 45 states produce five *LS* terms, whose properties are summarized in Tab. 1. In that table the standard ^{2S+1}L notation is used, where S and L stand for the total spin and orbital momenta, respectively. These five terms make the energy level scheme of a free ion.

The free ion's energy levels split, when such an ion is placed into a crystal field. The splitting pattern depends on the symmetry properties of the crystal lattice site occupied by an impurity ion. An analysis of the energy levels schemes of the TM ions in crystal field of cubic symmetry can be performed with the help of the so-called Tanabe-Sugano diagrams[12]. Three main parameters are needed for this purpose: the crystal-field strength Dq (which describes the crystal field effects), and two Racah parameters B and C (which determine the energy intervals between the free ion terms due to the Coulomb interaction between the electrons in the unfilled electron shell). The horizontal axis in all such diagrams is the Dq/B ratio, the vertical axis is the energy E of the split states in terms of the Racah parameter B (or the E/B ratio), and the diagrams are plotted for a fixed C/B ratio.

Fig. 1 depicts the Tanabe-Sugano diagram for a $3d^8$ ion in an octahedral crystal field.

Tab. 1 Symbols, degeneracy and energies of the *LS* terms of the $3d^8$ electron configuration. The ground term energy is taken as zero

Term symbols	Orbital degeneracy $2L+1$	Total degeneracy $(2L+1)\times(2S+1)$	Energy (in terms of Racah parameters B, C)
^3F (L=3)	7	21	0
^3P (L=1)	3	9	$15B$
^1D (L=2)	5	5	$5B + 2C$
^1G (L=4)	9	9	$12B + 2C$
^1S (L=0)	1	1	$22B + 7C$

When Dq/B ratio is equal to zero, the free ion's energy level scheme is restored. When $Dq/B>0$, the energy levels are split, and the split levels depend on the Dq/B value. It can be noted, however, that

the energy separation between the ground state spin-triplet $^3A_2$ and the first spin-singlet ^1E state is practically independent of the crystal-field strength. Moreover, at some Dq/B value the first excited spin-triplet state $^3T_2$ and the first spin-singlet ^1E intersect with each other. This allows to consider two special cases: (1) a weak crystal-field, where the first excited state $^3T_2$ originates from the same ^3F term as the ground state $^3A_2$ and, (2) a strong crystal-field, where the first excited state is ^1E, which comes from the ^1D term of a free ion. The Dq/B value, at which the energies of the $^3T_2$ and ^1E states are equal, is a separation between these two situations, as shown by a vertical dashed line in Fig. 1.

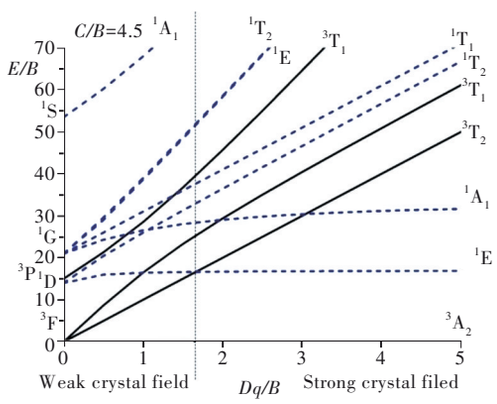

Fig.1　Tanabe-Sugano diagram for anion with the $3d^8$ electron configuration in an octahedral crystal-field. The spin-triplet and spin-singlet states are shown by the solid and dashed lines, respectively.

Since the energy of the ^1E state is very close to that of the ^1D free ion's term, it is possible to assume that only two Racah parameters B and C are needed to describe its energy position. The Racah parameters of the TM ions in crystals are considerably reduced relative to their "free ion" counterparts due to the so-called nephelauxetic effect[13]; the degree of such a reduction depends on the peculiarities of the chemical bonds between the TM ions and ligands. The Racah parameters are reduced greatly in the covalent crystals, and their reduction is not so pronounced in the ionic compounds. As a result, the ^1E state will be lowered in covalently bonded systems and will be located higher in ionic crystals.

This observation allowed to introduce a new parameter β_1 to the description of the spin-forbidden transitions[14-20]. It has been shown that the energy of the spin-doublet ^2E of the Mn^{4+} and Cr^{3+} ions (or the ^1E state of the Ni^{2+} ions) is a linear function of this new parameter $\beta_1 = \sqrt{\left(B/B_0\right)^2 + \left(C/C_0\right)^2}$ (where B and C are the Racah parameters in the crystal and B_0 and C_0 are the corresponding free ion's values). In the present paper we give an extended overview of the Ni^{2+} spectroscopic properties (in the octahedral coordination), based on the recent publications, and demonstrate this linear behavior.

The collected in the present paper experimental data on the Ni^{2+}-doped solids provide a valuable source of reference information for the experimentalists, whereas the established linear trend between the ^1E level position and new parameter β_1 allows for a meaningful estimation of the Ni^{2+} spectroscopic properties in new hosts.

2　Analysis of Spectroscopic Data on The Spin-forbidden $^3A_2 \rightarrow {}^1E$ Absorption Transition of Ni^{2+} Ions in Solids

Tab. 2 contains the values of the Racah parameters B and C for Ni^{2+} ions in various solids. In addition, the energetical positions of the Ni^{2+} ^1E state (calculated from the crystal field theory) and measured experimentally are also listed, along with the corresponding literature references.

Tab. 2　The main spectroscopic parameters related to the Ni^{2+} $^3A_2 \rightarrow {}^1E$ transition in various crystalline solids. $\beta_1 = \sqrt{\left(B/B_0\right)^2 + \left(C/C_0\right)^2}$, B_0=1 068 cm^{-1}, C_0=4 457 cm^{-1}[21]

Crystal	B/cm^{-1}	C/cm^{-1}	β_1	Position of the ^1E level/cm^{-1}			Ref.
				Calculated	Experimental	Calc., Eq.(1)	
AgBr	708	2 615	0.885 27	10 223	10 700	10 765	[22]
AgCl	807	3 141	1.033 25	12 206	12 470	12 411	[23]
Al_2O_3	900	4 250	1.272 56	15 009	15 840	15 072	[24]
β-BaB_2O_4	850	3 500	1.118 08	13 351	—	13 354	[25]
$BaLiF_3$	1 062	3 865	1.319 39	15 504	15 504	15 593	[26]

Tab.2(continue)

Crystal	B/cm^{-1}	C/cm^{-1}	β_1	Position of the ^{1}E level/cm^{-1}			Ref.
				Calculated	Experimental	Calc., Eq.(1)	
$Ca_3Sc_2Ge_3O_{12}$	935	3 503	1.176 51	13 841	—	14 004	[27]
$CdBr_2$	675	2 975	0.919 24	11 963	12 104	11 143	[28]
$CdCl_2$	750	3 150	0.996 32	13 147	13 065	12 000	[28]
CdI_2	730	3 450	1.032 65	12 419	12 450	12 404	[29]
$CsCdBr_3$	776	3 041	0.996 39	11 781	11 780	12 001	[30]
$CsCdCl_3$	799	3 142	1.027 67	12 132	12 700	12 349	[31]
$CsMgBr_3$	782	3 026	0.998 54	11 800	11 800	12 025	[30]
$CsMgBr_3$	886	3 952	1.214 27	14 555	14 700	14 424	[32]
$CsMgCl_3$	868	3 869	1.189 15	14 435	—	14 145	[32]
$CsMgI_3$	879	3 918	1.204 22	14 346	—	14 312	[32]
$KMgF_3$	950	3 990	1.262	15 247	15 156	14 955	[33]
$KNiF_3$	952	4 188	1.295 18	15 002	15 454	15 324	[34]
$KZnF_3$	880	3 696	1.169 01	13 891	-	13 921	[35]
K_2ZnF_4	1 028	3 794	1.284 96	15 061	15 313	15 210	[36]
LiCl	830	3 980	1.183 8	14 048	14 330	14 085	[37]
$LiGa_5O_8$	881	3 225	1.097 29	12 986	12 987	13 123	[23]
α-$LiIO_3$	913	4 069	1.250 71	15 304	—	14 829	[38]
$LiNbO_3$	816	3 224	1.052 15	12 120	12 120	12 621	[39]
$MgAl_2O_4$	865	3 254	1.090 42	13 002	12 987	13 047	[40]
$MgBr_2$	800	3 200	1.037 58	12 274	12 200	12 459	[41]
MgF_2	995	4 192	1.323 85	15 583	15 600	15 643	[23]
$MgGa_2O_4$	869	3 150	1.077 76	12 814	12 870	12 906	[42]
MgO	935	3 330	1.150 94	13 196	13 535	13 720	[43]
$20MoO_3$-$80TeO_2$	780	3 675	1.101 48	13 222	13 440	13 170	[44]
$Ni_3(BO_3)_2$, 2a site	915	3 797	1.208 21	9 611	—	14 357	[45]
$Ni_3(BO_3)_2$, 4f site	871	2 964	1.052 31	8 728	—	12 623	[45]
$NiBr_2$	763	2 772	0.947 21	12 550	—	11 454	[46]
$NiCl_2$	785	4 045	1.167 87	13 907	13 800	13 908	[46]
$NiCl_2(H_2O)_4$	928	3 764	1.211 7	14 359	14 803	14 395	[47]
NiF_2	697	4 035	1.116 03	13 799	—	13 331	[48]
NiI_2	646	3 851	1.054 71	11 171	11 165	12 649	[46]
$RbCaF_3$	1 034	3 816	1.292 44	15 040	15 000	15 293	[49]
$RbCdF_3$	950	4 000	1.263 6	14 075	—	14 972	[50]
WO_3-TeO_2	958	3 330	1.167 4	13 831	—	13 903	[51]
ZAS	940	3 919	1.244 11	14 124	14 124	14 756	[52]
ZLKB1	770	3 250	1.025 44	12 294	12 269	12 324	[53]
ZLKB2	765	3 200	1.014 18	12 126	12 162	12 199	[53]
ZLKB3	770	3 260	1.027 03	12 284	12 315	12 342	[53]
ZLKB4	790	3 250	1.038 69	12 404	12 419	12 471	[53]
ZLKB5	790	3 200	1.030 84	12 308	12 311	12 384	[53]
ZLNB1	780	3 250	1.032 04	12 334	12 297	12 397	[54]
ZLNB2	795	3 290	1.048 33	12 521	12 623	12 578	[54]
ZLNB3	800	3 285	1.050 87	12 544	12 575	12 607	[54]
ZLNB4	810	3 285	1.057 56	12 614	12 623	12 681	[54]
ZLNB5	810	3 285	1.057 56	12 616	12 575	12 681	[54]
ZnF_2	972	3 586	1.214 76	14 162	—	14 429	[55]
ZnO-CdS nanocomposite	820	3 250	1.058 88	12 621	12 626	12 696	[56]
$ZnSiF_6 \cdot 6H_2O$	932	4 155	1.276 95	15 239	—	15 121	[57]

Notes: The chemical compositions of the glasses listed in the table are as follows: ZAS glass: $58SiO_2 + 21ZnO + 10Al_2O_3 + 5TiO_2 + 3Ga_2O_3 + 3K_2O$; ZLKB1: $19.9ZnO + 5Li_2O + 25K_2O + 50B_2O_3 + 0.1NiO$; ZLKB2: $19.9ZnO + 10Li_2O + 20K_2O + 50B_2O_3 + 0.1NiO$; ZLKB3: $19.9ZnO + 15Li_2O + 15K_2O + 50B_2O_3 + 0.1NiO$; ZLKB4: $19.9ZnO + 20Li_2O + 10K_2O + 50B_2O_3 + 0.1NiO$; ZLKB5: $19.9ZnO + 25Li_2O + 5K_2O + 50B_2O_3 + 0.1NiO$; ZLNB1: $19.9ZnO + 5Li_2O + 25Na_2O + 50B_2O_3 + 0.1NiO$; ZLNB2: $19.9ZnO + 10Li_2O + 20Na_2O + 50B_2O_3 + 0.1NiO$; ZLNB3: $19.9ZnO + 15Li_2O + 15Na_2O + 50B_2O_3 + 0.1NiO$; ZLNB4: $19.9ZnO + 20Li_2O + 10Na_2O + 50B_2O_3 + 0.1NiO$; ZLNB5: $19.9ZnO + 25Li_2O + 5Na_2O + 50B_2O_3 + 0.1NiO$.

It is easy to see from the data presented in Tab. 1 that all listed parameters vary in wide ranges. Thus, the value of B varies from 646 cm^{-1} in NiI_2 to 1 062 cm^{-1} in $BaLiF_3$, the value of C changes from 2 615 cm^{-1} in AgBr to 4 250 cm^{-1} in Al_2O_3 and the energy of the ^1E state is in between 10 700 cm^{-1} in AgBr and 15 840 cm^{-1} in Al_2O_3.

Such wide limits can be explained by differences in chemical bonding: in highly covalent iodides and bromides the nephelauxetic effect is strong and the Racah parameters are reduced considerably. At the same time, the highly ionic fluorides are characterized by a weaker nephelauxetic effect and, correspondingly, greater values of the Racah parameters. Therefore, the degree of covalency of the chemical bonds between the Ni^{2+} ions and ligands is the primary reason for the observed variations of the spectroscopic parameters in Tab. 1. The data in the "calculated" column correspond to the values obtained from the Tanabe-Sugano matrices in the cubic crystal field approximation. Since the Ni^{2+} sites very often are characterized by a lower symmetry (trigonal or tetragonal), such calculated values can deviate from the experimental data.

Fig. 2 shows the variation of the experimental positions of the Ni^{2+} ^1E state against the $\beta_1 = \sqrt{\left(B/B_0\right)^2 + \left(C/C_0\right)^2}$ parameter.

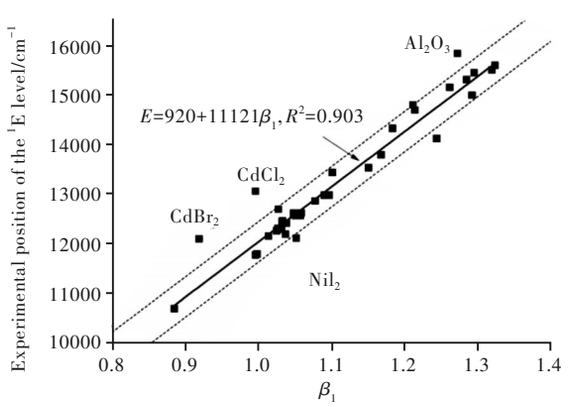

Fig.2　Experimental position of the Ni^{2+} ^1E state(symbols) *versus* the $\beta_1 = \sqrt{\left(B/B_0\right)^2 + \left(C/C_0\right)^2}$ parameter. The solid line is the fit to the experimental data, the dashed lines are shifted up-/down-ward by 407 cm^{-1}, which is the root-mean-squared deviation between the fit line and experimental data. See text for further details.

The data points were fitted to the linear function

$$E(^1E) = 920 + 11121\beta_1, \qquad (1)$$

the value of the correlation coefficient R^2 is rather high (0.903), which indicates a good quality of the fit.

To assess the quality of the fit and variance of the data presented, we calculated the energy of the Ni^{2+} ^1E state using Eq. (1) in the various compounds that are listed in Tab. 1 and then determined the root-mean-squared deviation

$$\sigma = \sqrt{\frac{\sum_{i=1}^{N}\left(E_{i(\mathrm{exp.})} - E_{i(\mathrm{Eq.(1)})}\right)^2}{N}}, \qquad (2)$$

where $E_{i(\mathrm{exp.})}$ and $E_{i(\mathrm{Eq.\ (1)})}$ are the corresponding experimental value and the calculated with the help of Eq. (1). The numerical estimations returned the value σ=407 cm^{-1}. Two dashed straight lines in Fig. 1 are parallel to the fit line (Eq. (1)) and correspond to its upward/downward shift by the value of σ. It should be noted that this value is of the order of magnitude of the phonon frequencies on solids and practically all data points in Fig. 1 are within the $\pm\sigma$ interval from the fit line. However, some data points, which correspond to NiI_2, $CdBr_2$, $CdCl_2$, Al_2O_3 compounds are outside of that area. The first three halides in this group are characterized by a layered structure and the chemical bonds are highly covalent.

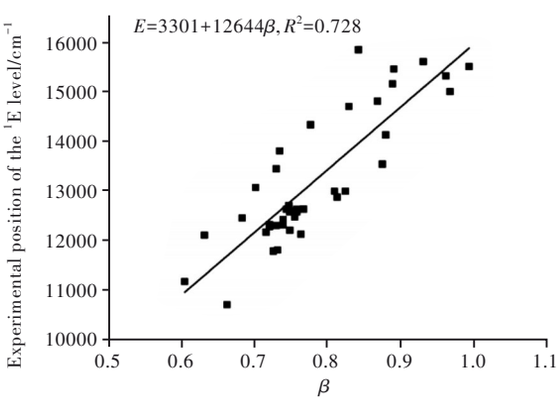

Fig.3　Energy position of the Ni^{2+} ^1E state (symbols) against the $\beta = B/B_0$ parameter

To illustrate the validity of our choice of the $\beta_1 = \sqrt{\left(B/B_0\right)^2 + \left(C/C_0\right)^2}$ parameter, we also show in Fig. 3 the dependence of the experimental energy position of the Ni^{2+} ^1E state on the "old" nephelauxetic

ratio $\beta = B/B_0$, which for a long time was considered as a qualitative measure of covalency. It can be easily seen from Fig. 3, that the data points are much more scattered than in Fig. 2. The linear fit returns a much smaller value of the correlation coefficient (only 0.728). A similar result was obtained by us when considering the Mn^{4+} ions and dependence of their ^2E level on the same parameter. Therefore, consideration of only one parameter B for the covalency description is insufficient, and both Racah parameters B and C have to be used when relating the energies of the spin-forbidden transitions of the TM ions chemical bonds covalency. Moreover, the present empirical finding has been confirmed and supported by our theoretical derivation based on the parameterized Tanabe-Sugano formula of ^1E energy level position of $3d^8$ ions in octahedral complexes, as shown by Ref. [19].

We note that the linear relation between the ^1E level and β_1 parameter holds true for the zero-phonon transitions. Quite often identification of the zero-phonon line(ZPL) position in the TM ions spectra is not an easy task, since the Stokes and anti-Stokes vibronic progressions that are observed in the experimental emission/absorption spectra can mask the true ZPL position. We consider this as an important factor that can cause deviation of some experimental data points in Fig. 2 from the straight line determined by Eq. (1). In addition, such a linear relation can be also expected to be held for the case of $3d^2$ ions in tetrahedral complexes because of the electron-hole complementarity between both $3d^8$ and $3d^2$ electronic configurations.

3 Conclusion

A thorough analysis of the recent publications on the spectroscopic properties of solids doped with Ni^{2+} ions allowed to compile a database that collects the values of the Racah parameters B, C and energetic positions of the Ni^{2+} ^1E level. We have re-examined an empirical trend between the lowest energy spin-forbidden Ni^{2+} $^3A_2$-^1E transition and a new covalency parameter $\beta_1 = \sqrt{\left(B/B_0\right)^2 + \left(C/C_0\right)^2}$, which allows to account for a decrease of both Racah parameters because of nephelauxetic effect. The β_1 parameter describes the covalent effects much better than the commonly used nephelauxetic ratio $\beta = B/B_0$, which omits the second Racah parameter, C. It is hoped that the collected in the present paper data and their treatment will be useful for the description of the spectroscopic properties of Ni^{2+} ions in solids.

Response Letter is available for this paper at: http://cjl.lightpublishing.cn/thesisDetails#10.37188/CJL.20220243.

References:

[1] POWELL R C. *Physics of Solid-state Laser Materials* [M]. New York: Springer, 1998.

[2] AVRAM N M, BRIK M G. *Optical Properties of 3d-ions in Crystals: Spectroscopy and Crystal Field Analysis* [M]. Beijing: Tsinghua University Press, 2013.

[3] BRIK M G, MA C G. *Theoretical Spectroscopy of Transition Metal and Rare Earth Ions: From Free State to Crystal Field* [M]. New York: Jenny Stanford Publishing, 2020.

[4] KÜCK S. Laser-related spectroscopy of ion-doped crystals for tunable solid-state lasers [J]. *Appl. Phys.* B, 2001, 72(5): 515-562.

[5] LIU R S, WANG X J. *Phosphor Handbook: Experimental Methods for Phosphor Evaluation and Characterization* [M]. 3rd ed. London: CRC Press, 2022.

[6] SETLUR A A, RADKOV E V, HENDERSON C S, *et al*. Energy-efficient, high-color-rendering LED lamps using oxyfluoride and fluoride phosphors [J]. *Chem. Mater.*, 2010, 22(13): 4076-4082.

[7] SRIVASTAVA A M, SOULES T F. *Luminescent materials (Phosphors)* [M]. Kirk-Othmer Eds. *Kirk-Othmer Encyclopedia of Chemical Technology*. 4th ed. Vol. 15. New York: John Wiley & Sons, 1995.

[8] ZHOU Q, DOLGOV L, SRIVASTAVA A M, *et al.* Mn^{2+} and Mn^{4+} red phosphors: synthesis, luminescence and applications in WLEDs. A review [J]. *J. Mater. Chem.* C, 2018, 6(11): 2652-2671.

[9] NIE J M, LI Y, LIU S S, *et al.* Tunable long persistent luminescence in the second near-infrared window via crystal field control [J]. *Sci. Rep.*, 2017, 7(1): 12392-1-7.

[10] MATUSZEWSKA C, MARCINIAK L. The influence of host material on NIR Ⅱ and NIR Ⅲ emitting Ni^{2+} based luminescent thermometers in $ATiO_3:Ni^{2+}$ (A=Sr, Ca, Mg, Ba) nanocrystals [J]. *J. Lumin.*, 2020, 223: 117221-1-9.

[11] GAO Y, WANG B N, LIU L, *et al.* Near-infrared engineering for broad-band wavelength-tunable in biological window of NIR-Ⅱ and -Ⅲ: a solid solution phosphor of $Sr_{1-x}Ca_xTiO_3:Ni^{2+}$ [J]. *J. Lumin.*, 2021, 238: 118235-1-7.

[12] SUGANO S, TANABE Y, KAMIMURA H. *Multiplets of Transition-metal Ions in Crystals* [M]. New York: Academic Press, 1970.

[13] FIGGIS B N, HITCHMAN M A. *Ligand Field Theory and Its Applications* [M]. New York: Wiley-VCH, 2000.

[14] BRIK M G, SRIVASTAVA A M. Electronic energy levels of the Mn^{4+} Ion in the perovskite, $CaZrO_3$ [J]. *ECS J. Solid State Sci. Technol.*, 2013, 2(7): R148-R152.

[15] SRIVASTAVA A M, BRIK M G. Crystal field studies of the Mn^{4+} energy levels in the perovskite, $LaAlO_3$ [J]. *Opt. Mater.*, 2013, 35(8): 1544-1548.

[16] BRIK M G, SRIVASTAVA A M, AVRAM N M, *et al.* Empirical relation between covalence and the energy position of the Ni^{2+} ^1E state in octahedral complexes [J]. *J. Lumin.*, 2014, 148: 338-341.

[17] BRIK M G, CAMARDELLO S J, SRIVASTAVA A M. Influence of covalency on the Mn^{4+} $^2E_g \rightarrow {}^4A_{2g}$ emission energy in crystals [J]. *ECS J. Solid State Sci. Technol.*, 2015, 4(3): R39-R43.

[18] BRIK M G, CAMARDELLO S J, SRIVASTAVA A M, *et al.* Spin-forbidden transitions in the spectra of transition metal ions and nephelauxetic effect [J]. *ECS J. Solid State Sci. Technol.*, 2016, 5(1): R3067-R3077.

[19] MA C G, WANG Y, LIU D X, *et al.* Origin of the β_1 parameter describing the nephelauxetic effect in transition metal ions with spin-forbidden emissions [J]. *J. Lumin.*, 2018, 197: 142-146.

[20] BRIK Mikhail G, 马崇庚, SRIVASTAVA Alok M, 等. 用于固态照明的Mn^{4+}离子光谱学 [J]. 发光学报, 2020, 41(9): 1011-1029.
BRIK M G, MA C G, SRIVASTAVA A M, *et al.* Mn^{4+} ions for solid state lighting [J]. *Chin. J. Lumin.*, 2020, 41(9): 1011-1029. (in English)

[21] UYLINGS P H M, RAASSEN A J J, WYART J F. Energies of N equivalent electrons expressed in terms of two-electron energies and independent three-electron parameters: a new complete set of orthogonal operators: Ⅱ. Application to $3d^N$ configurations [J]. *J. Phys.* B: *At. Mol. Phys.*, 1984, 17(20): 4103-4126.

[22] WANG H Q, KUANG X Y, LI H F. EPR and optical spectra of Ni^{2+}-V_{Ag} in silver chloride and silver bromide [J]. *Mol. Phys.*, 2009, 107(7): 621-627.

[23] BRIK M G, AVRAM C N, AVRAM N M. Comparative study of crystal field effects for Ni^{2+} ion in $LiGa_5O_8$, MgF_2 and AgCl crystals [J]. *J. Phys. Chem. Solids*, 2008, 69(7): 1796-1801.

[24] FANG W, WANG Q W, YANG W Y, *et al.* Theoretical studies of EPR parameters and defect structures for Ni^{2+} ions in corundum [J]. *Phys.* B *Condens. Matter*, 2013, 408: 169-174.

[25] REDDY V, KRISHNA R, RAO T R, *et al.* Synthesis and optical properties of Co^{2+} and Ni^{2+} ions doped β-BaB_2O_4 nanopowders [J]. *J. Lumin.*, 2012, 132(9): 2325-2329.

[26] ANDREICI E L, AVRAM N M. Fine structure of optical energy levels scheme for Ni^{2+} doped in inverted perovskite $BaLiF_3$ [J]. *AIP Conf. Proc.*, 2011, 1387: 155-159.

[27] BRIK M G. Crystal field analysis of the absorption spectra and electron-phonon interaction in $Ca_3Sc_2Ge_3O_{12}:Ni^{2+}$ [J]. *J. Phys. Chem. Solids*, 2006, 67(4): 738-744.

[28] ACKERMAN J, FOUASSIER C, HOLT E M, *et al.* 5. deg. Crystal spectra of nickel(Ⅱ) chloride and nickel(Ⅱ) bromide [J]. *Inorg. Chem.*, 1972, 11(12): 3118-3122.

[29] BRIK M G, KITYK I V, OZGA K, *et al.* Structural, electronic and optical properties of pure and Ni^{2+}-doped CdI_2 layered crystals as explored by *ab initio* and crystal field calculations [J]. *Phys.* B *Condens. Matter*, 2011, 406(2): 192-199.

[30] WENGER O S, BÉNARD S, GÜDEL H U. Crystal field effects on the optical absorption and luminescence properties of Ni^{2+}-doped chlorides and bromides: crossover in the emitting higher excited state [J]. *Inorg. Chem.*, 2002, 41(23):

5968-5977.

[31] OETLIKER U, RILEY M J, GÜDEL H U. Excited state spectroscopy of Ni^{2+} doped chloride and fluoride lattices [J]. *J. Lumin.*, 1995, 63(1-2): 63-73.

[32] FENG W L, CHEN J J, HAN Z. Investigations of the optical and EPR spectra for $(NiX_6)^{4-}$ (X=Cl, Br, I) clusters [J]. *J. Magn. Magn. Mater.*, 2009, 321(19): 3290-3292.

[33] FERGUSON J, GUGGENHEIM H J, WOOD D L. Electronic absorption spectrum of Ni Ⅱ in cubic perovskite fluorides. Ⅰ [J]. *J. Chem. Phys.*, 1964, 40(3): 822-830.

[34] BARREDA-ARGÜESO J A, RODRÍGUEZ F. Pressure dependence of the crystal-field spectrum of $KNiF_3$: Single and double excitations [J]. *Phys. Rev. B*, 2021, 103(8): 085115-1-9.

[35] BRIK M G, KUMAR G A, SARDAR D K. *Ab initio*, crystal field and experimental spectroscopic studies of pure and Ni^{2+}-doped $KZnF_3$ crystals [J]. *Mater. Chem. Phys.*, 2012, 136(1): 90-102.

[36] WANG S J, KUANG X Y, LU C. Theoretical study of local structure for Ni^{2+} ions at tetragonal sites in K_2ZnF_4: Ni^{2+} system [J]. *Spectrochim. Acta A Mol. Biomol. Spectrosc.*, 2008, 71(4): 1317-1320.

[37] FANG W, TANG H Y, CHENG W D, *et al*. Theoretical investigations of optical spectra and electron paramagnetic resonance spectra of LiCl: Ni^{2+} crystals [J]. *Spectrochim. Acta A Mol. Biomol. Spectrosc.*, 2012, 99: 342-346.

[38] FENG W L, ZHENG W C. Studies of the defect structure from the calculations of optical and electron paramagnetic resonance spectra for Ni^{2+} centre in α-$LiIO_3$ crystal [J]. *Pramana*, 2008, 71(3): 573-578.

[39] YANG Z Y, RUDOWICZ C, YEUNG Y Y. Microscopic spin-Hamiltonian parameters and crystal field energy levels for the low C_3 symmetry Ni^{2+} centre in $LiNbO_3$ crystals [J]. *Phys.* B *Condens. Matter*, 2004, 348(1-4): 151-159.

[40] BRIK M G, AVRAM N M, AVRAM C N, *et al*. Ground and excited state absorption of Ni^{2+} ions in $MgAl_2O_4$: crystal field analysis [J]. *J. Alloys Compd.*, 2007, 432(1-2): 61-68.

[41] GONZÁLEZ E, RODRIGUE-WITCHEL A, REBER C. Absorption spectroscopy of octahedral nickel (Ⅱ) complexes: a case study of interactions between multiple electronic excited states [J]. *Coord. Chem. Rev.*, 2007, 251(3-4): 351-363.

[42] ANDREICI E L, STANCIU M, AVRAM N M. Crystal field studies on $MgGa_2O_4$: Ni^{2+} [J]. *AIP Conf. Proc.*, 2010, 1262(1): 130-135.

[43] MIRONOVA-ULMANE N, BRIK M G, SILDOS I. Crystal field calculations of energy levels of the Ni^{2+} ions in MgO [J]. *J. Lumin.*, 2013, 135: 74-78.

[44] ZAMYATIN O A, CHURBANOV M F, PLOTNICHENKO V G, *et al*. Optical properties of the MoO_3-TeO_2 glasses doped with Ni^{2+} ions [J]. *J. Non-Cryst. Solids*, 2018, 480: 74-80.

[45] MOLCHANOVA A D. Experimental study and analysis of absorption spectra of Ni^{2+} ions in nickel orthoborate $Ni_3(BO_3)_2$ [J]. *Phys. Solid State*, 2018, 60(10): 1957-1965.

[46] BRIK M G, AVRAM N M, AVRAM C N. Comparative crystal field study of Ni^{2+} energy levels in $NiCl_2$, $NiBr_2$, and NiI_2 crystals [J]. *Phys.* B *Condens. Matter*, 2006, 371(1): 43-49.

[47] KAMMOUN S, DAMMAK M, MAALEJ R, *et al*. Crystal-field analysis for d^8 ions at D_{4h} symmetry sites: Electronic states in *trans*-$NiCl_2(H_2O)_4$ complex [J]. *J. Lumin.*, 2007, 124(2): 316-320.

[48] ZHAO M G, DU M L. Determination of the state equation of NiX_2 from the high-pressure spectra shifts [J]. *J. Phys.* C: *Solid State Phys.*, 1987, 20(28): 4467-4475.

[49] LI H F, KUANG X Y, WANG H Q. Local structural properties of $(NiF_6)^{4-}$ clusters in perovskite fluorides $RbMF_3$ (M = Cd^{2+}, Ca^{2+}, Mg^{2+}) series: EPR and optical spectra study in tetragonal and trigonal ligand field [J]. *Chem. Phys. Lett.*, 2008, 462(1-3): 133-137.

[50] ALCALA R, CASAS GONZALEZ J, VILLACAMPA B, *et al*. Photoluminescence of Ni^{2+} ions in $RbCdF_3$ and $RbCaF_3$ [J]. *J. Lumin.*, 1991, 48-49: 569-573.

[51] PLOTNICHENKO V G, SOKOLOV V O, SNOPATIN G E, *et al*. Optical absorption and structure of impurity Ni^{2+} center in tungstate-tellurite glass [J]. *J. Non-Cryst. Solids*, 2011, 357(3): 1070-1073.

[52] SUZUKI T, HORIBUCHI K, OHISHI Y. Structural and optical properties of ZnO-Al_2O_3-SiO_2 system glass-eramics containing Ni^{2+}-doped nanocrystals [J]. *J. Non Cryst. Solids*, 2005, 351(27-29): 2304-2309.

[53] KUMARI G K, BEGUM M, KRISHNA R, *et al*. Physical and optical properties of Co^{2+}, Ni^{2+} doped $20ZnO+xLi_2O+(30-x)K_2O+50B_2O_3$ ($5 \leqslant x \leqslant 25$) glasses: observation of mixed alkali effect [J]. *Mater. Res. Bull.*, 2012, 47(9): 2646-2654.

[54] RAO T R, KRISHNA R, VENKATA REDDY C H V*et al.* Mixed alkali effect and optical properties of Ni^{2+} doped 20ZnO+$x$$Li_2O$+(30−$x$)$Na_2O$+50$B_2O_3$ glasses [J]. *Spectrochim. Acta* A *Mol. Biomol. Spectrosc.*, 2011, 79(5): 1116-1122.

[55] WANG S J, KUANG X Y, DUAN M L, *et al.* Comparative study of EPR spectra and crystal field effect on local structure for $(NiF_6)^{4-}$ coordination complex in Ni^{2+}:ZnF_2, NiF_2, and Ni^{2+}:MgF_2 systems [J]. *Phys. Status Sol.* B, 2010, 247(2): 416-421.

[56] GURUGUBELLI T R, RAVIKUMAR R V S S N, KOUTAVARAPU R. Structural, optical, and luminescence properties of Ni^{2+} doped ZnO-CdS nanocomposite: synthesis and investigations for green light emission [J]. *Chem. Papers*, 2022, 76(1): 557-566.

[57] LI C G, KUANG X Y, ZHAO Y R, *et al.* Investigation of the local structure and ZFS parameter for Ni^{2+} (V^{2+}) ions in zinc fluosilicate at different pressure [J]. *Chem. Phys. Lett.*, 2011, 512(4-6): 263-268.

BRIK Mikhail G (1969 −), received his PhD from Kuban State University (Russia) in 1995 and his DSc (habilitation) from the Institute of Physics, Polish Academy of Sciences (Poland) in 2012. Since 2007 he is a professor at the Institute of Physics, University of Tartu, Estonia. Before that, he worked at Kyoto University (Japan) from 2003 to 2007, Weizmann Institute of Science (Israel) in 2002, Asmara University (Eritrea) from 2000 to 2001, and Kuban State University from 1995 to 2000. He is also a distinguished visiting professor at Chongqing University of Posts and Telecommunications (China) and Professor at Jan Długosz University (Poland). Since 2015 he serves as one of the editors of *Optical Materials* (Elsevier). Prof. Brik's scientific interests cover theoretical spectroscopy of transition metal and rare earth ions in optical materials, crystal field theory, and *ab initio* calculations of the physical properties of pure and doped functional compounds. He is a coeditor of two books and author of 12 book chapters and about 410 papers in international journals. According to Google Scholar (June 2020), he has more than 8 500 citations with h index 45. He received the Dragomir Hurmuzescu Award of Romanian Academy in 2006 and the State Prize of the Republic of Estonia in the field of exact sciences in 2013. In 2018 he received the state professor title from the President of Poland.
E-mail: mikhail.brik@ut.ee

MA Chong-geng(1980−), received his PhD from University of Science and Technology of China in 2008. He spent three years (2010—2013) as a post-doctor in University of Tartu with the financial support of European Social Fund. He was also a visiting professor at University of Verona in 2017. His area of scientific interests covers the first-principles and crystal−field design of luminescent materials. He has published one book and more than 100 papers in international journals, which attracted more than 2 500 citations(h index=27). Currently he is a full professor and the director of CQUPT-BUL Innovation Institute at Chongqing University of Posts and Telecommunications.
E-mail: macg@cqupt.edu.cn

《发光学报》第13届编辑委员会委员名单

The 13th Editorial Committee of Chinese Journal of Luminescence

(2019—2023)